A New STOL Flying Boat Design

SHIZUO KIKUHARA* AND KOICHI TOKUDA†
Shin-Meiwa Industry Company Ltd., Japan

A four engined turboprop flying boat, the PX-S, gross weight (G.W.) 87,000 lb, with high open ocean capability has been designed and is under construction. The deflected slip stream and boundary-layer control (BLC) are adopted as high lift devices. Automatic stabilization equipment is included in the fully powered flight control system. A newly developed spray suppressor is applied on the hull forebody. A dynamically similar flying model, the UF-XS, 75% in linear dimension, was constructed and flight tested. The results show the following: the C_L measured at takeoff, 40 knots, is 6.9; a takeoff run with 18 knots of wind is about 400 ft in 10 sec; the low landing speed, 45 knots, together with an air cushion effect of the BLC near the surface makes the landing shock very small; the flying quality at low speeds, with automatic stabilization equipment on, is satisfactory except for a large side slip during approach caused by asymmetric force on the nacelles by the like-rotation propellers (this problem was almost solved in the SS-2 design, which is one of the model numbers, by lowering the nacelle position relative to the wing); the hull has a wide stable trim range and the spray characteristics are satisfactory. The estimated utilization of the SS-2 through the year in the North Pacific Ocean is 86%.

Nomenclature

C_L = lift coeff
C_l = rolling moment coeff
Cm = pitching-moment coeff
Cn = yawing moment coeff
$Cn_{\delta a}$ = $\partial Cn/\partial \delta a$
$Cn_{\delta r}$ = $\partial Cn/\partial \delta r$
C_Y = side-force coeff
C_μ = blowing momentum coeff
D = drag
g = gravity acceleration
Im = imaginary part of root
K_{sc} = stick canceller const
K_0, K_1 = ASE gain
L = lift
L_0 = lift produced by slip stream
N_p = yawing moment due to roll rate
Nr = yawing moment due to yaw rate
$N_{\delta r}$ = yawing moment due to rudder deflection
P = period
Δp = static pressure increment
q = dynamic pressure
Re = real part of root
S = wing area
T = wave period
$T'c$ = thrust ÷ (qS)
$T^{1/2}$ = time to half amplitude, negative means double
V = speed
W = airplane weight
w = nozzle width
α = angle of attack
β = angle of side slip
γ = path angle
δ = surface deflection
θ = pitch attitude
$\dot{\theta}$ = pitch rate
ϕ = roll attitude
$\dot{\phi}$ = roll rate

Subscripts

a = aileron
ASE = automatic stabilization equipment
e = elevator
f = flap
H = hull
p = pilot
r = rudder
w = wind
o = reference
∞ = general flow

Presented as Preprint 65-755 at the AIAA/RAeS/JSASS Aircraft Design and Technology Meeting, Los Angeles, Calif., November 15–18, 1965; submitted December 17, 1965. The authors want to express their thanks to the Maritime Staff Office, Japanese Defense Agency, Shin-Meiwa Industry Company Ltd. for their permission to publish the present paper, and to M. Kasuh and O. Sugahara for their assistance in preparing this paper. The authors would also like to mention with thanks that the U. S. Navy has been giving much assistance to the project.

* Director, Chief Engineer, Shin-Meiwa Industry Company Ltd. Member AIAA.

† Chief of Research and Development Department, Aircraft Division, Shin-Meiwa Industry Company Ltd.

Introduction

A NEW STOL flying boat, designated PX-S, with a high open ocean capability has been designed and the prototype is now under construction in Japan under the sponsorship of the Japan Maritime Self-Defence Force. The maximum gross weight is 87,000 lb which can be raised up to 99,000 lb as a growth potential. The engines are four T64-GE-10 [2850 eshp each] to drive propellers and one T58-GE-8 (1250 shp) to drive a BLC compressor. The present paper describes the aerodynamic and hydrodynamic as-

a)

b)

Fig. 1 a) UF-XS, with spray suppressor; b) UF-2, without spray suppressor.

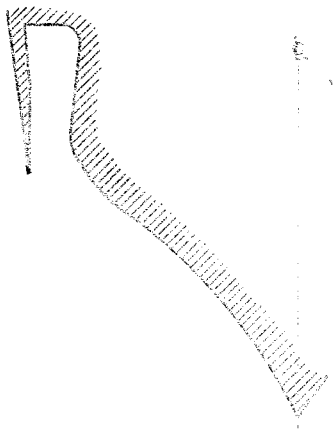

Fig. 2 Spray suppressor.

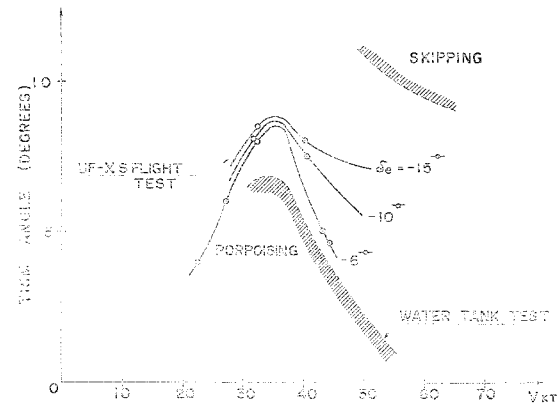

Fig. 4 Stability limit of trim, flap angle = 20°–15°, BLC off, c.g. = 24% mean aerodynamic chord (MAC).

pects of the design of the flying boat, referring to the actual flight test results of a three-quarter scale flying model, designated UF-XS.

Basic Design Concept

There are many water surfaces everywhere in the world, open oceans, inland seas, bays and lakes, all of which have a possibility to be flying boat bases provided the flying boat has a capability of takeoff and landing on high seas and of short time and run. The open ocean capability, therefore, is the key point in extending the utility boundaries of the flying boat to a much wider area than it has today.

In order to obtain a high open ocean capability, the following are essential: 1) low takeoff and landing speed, and short time and run; 2) good flying qualities at low speeds; 3) spray-free, stable, and low shock hull bottom; 4) ample reserve horsepower; and 5) high reliability of all the systems, equipments, and structures. Since the listed features must be realized without greatly sacrificing the general performances, i.e., range, payload, speed, climb, and so on, the following design techniques have been adopted: 1) the deflected slip stream and BLC system as the high lift device to obtain a usable C_L of 6 to 7 for takeoff and landing at 45 knots, keeping the wing loading at a moderately high value; 2) *ASE* for use at low speeds is included in a fully powered flight control mechanism with dual independent hydraulic systems; 3) a high length-to-beam ratio hull added with a newly developed spray control system,[1] the groove-type spray suppressor; and 4) light weight and powerful turboprop engines, four T64-GE-10's, to keep the power loading at a low value, 7.6 lb/eshp at maximum gross weight without unduly increasing the weight of the power plant.

Wind tunnels, towing tanks, computers, and flight simulators can afford the necessary data for design according to their own abilities, however they are separated. It is of the utmost importance to amalgamate them into a flying boat to achieve a successful design. For this purpose a three-quarter scale flying model, the UF-XS, was manufactured and flight tested before the final design of the PX-S was frozen.

Hydrodynamics

The hull has a high length-to-beam ratio of 11.7, and a dead rise angle of 23.5° at the step with warping of 6°/beam. It is provided with a groove-type spray suppressor along the chine of the hull forebody from the bow to the propeller-plane (Figs. 1–3). The water coming up along the bottom surface (Fig. 2) continues to cling to it along the rounded corner of the chine, leads into the longitudinal groove, flows rearward, and is thrown out of the exit (Fig. 3). An almost zero spray condition was realized in the towing tank test. The spray height measured in the actual test on the sea by the UF-XS was not zero, but very low (see Fig. 1a and 1b; compare the spray with a conventional flying boat). The stable region of the hull is wide enough (Fig. 4) and no porpoising or skipping was experienced on the UF-XS.

The impact loads on the hull in 10-ft waves are estimated below 3 g's through water tank tests and UF-XS flight tests (see also Fig. 5). The low shock value is caused by the low landing speed of 45 to 50 knots (with a 20-knot head wind the water speed is 25 to 30 knots), and an air cushion effect of the BLC blowing air near the ground (Fig. 3). No jumping was observed during the flight test; this is because the lift produced by engine power is cut down just after touch down, and hence the total lift is reduced rapidly to almost 20% of the airplane weight (Fig. 6).

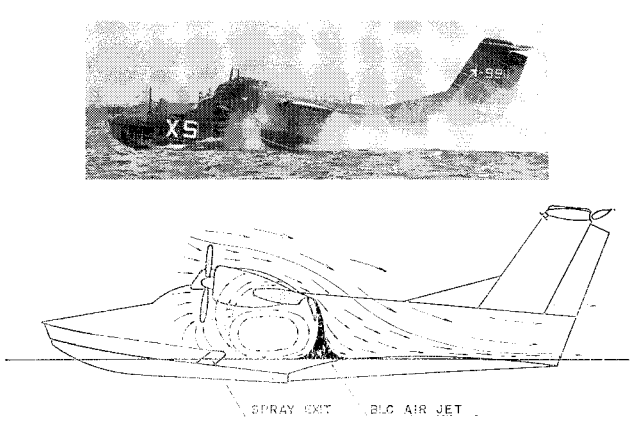

Fig. 3 Flow pattern during takeoff, UF-XS.

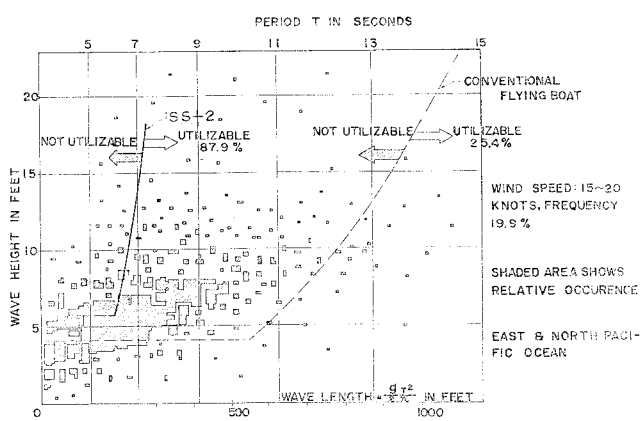

Fig. 5 Occurence probability of sea state in 15–20 knots wind and utilizable envelopes for takeoff and landing.

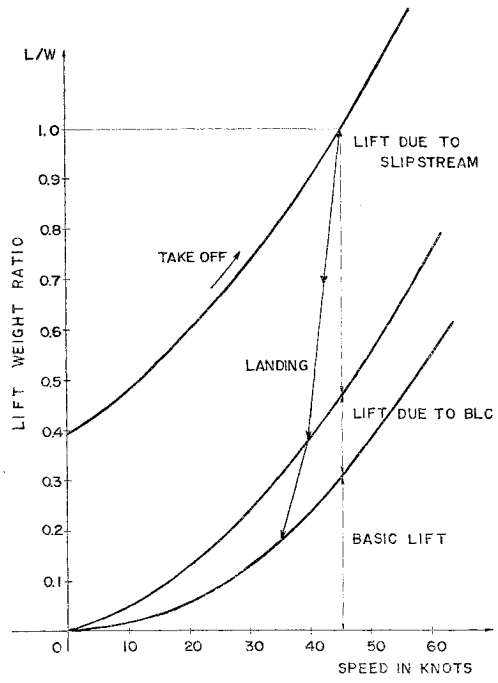

Fig. 6 Break down of lift, flap angle = 60-45-0, hull attitude = 7.

The tip floats have ample capacity and, together with reversible propellers, the SS-2 will have satisfactory maneuverability in the open ocean under 25-knot winds, and 37-knot gusts. Spray mist appeared at the takeoff run with BLC [Fig. 3 (top)]. It disappears when the airspeed reaches about 35 knots. This phenomenon was the one that was unexpected. The cause of the spray mist is understood by Fig. 3 (bottom), which was prepared through a wind-tunnel test with ground board and direct observations of the flight test.

Aerodynamics

High Lift Device

A low pressure blowing type BLC was adopted on the UF-XS, and the compressed air temperature was kept below about 200° F even in hot days in order to avoid the thermal deformation of the duct system and the adjacent structures. The power plant is two T58-GE-6 turboshaft engines that provide more than enough power for test purposes. Each engine drives an axial flow compressor specially designed for the purpose. Both the flap blowing and the shroud blowing types were tested, as shown in Table 1, to compare the relative merit of the two types.

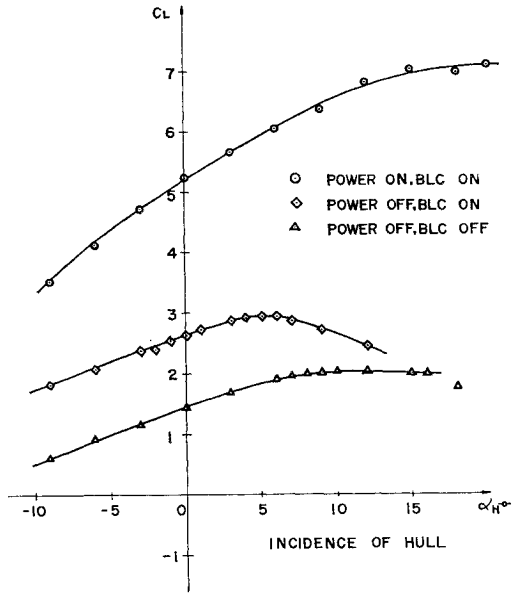

Fig. 7 Lift at takeoff configuration (wind-tunnel test of UF-XS), flap angle = 60-45-30 (wing setting angle = 5).

Table 1 C_μ and nozzle width[a]

	SS-2		UF-XS	
	C_μ[d]	w	C_μ	w_1
Inboard flaps	0.10	0.07 in. (F)	0.15	0.15, in (F)
Outboard flaps	0.10	0.07 (F)	0.15	0.10 (S)
Ailerons	...[c]	...	0.06	0.03 (S)
Elevators	0.05	0.04 (F)	0.15	0.07 (S)
Rudder	0.03	0.04 (F)	0.04	0.96 (F)
Pressure ratio[b]		1.85		1.60

[a] C_μ = (Jet momentum/q_∞ × area concerned), at 45 knots; w = nozzle width in inches; F = flap blowing type; and S = Shroud blowing type.
[b] At compressor exit.
[c] Not applied because the aileron drooping was canceled by the flight test results.
[d] Correspond to C_μ critical.

The flight test results are: 1) no thermal deformation was observed, 2) blowing above the C_μ critical is not worthwhile, and 3) the flap blowing type is better both aerodynamically and structurally. According to the test results of the UF-XS, the flap blowing type is adopted for all the surfaces on the SS-2, as shown in Table 1. The values of C_μ in the table correspond to C_μ critical. The power plant is one T58-GE-8 (1250 shp), driving a new axial compressor.

Figure 7 shows the C_L measured in the wind tunnel with an 8% powered model of the UF-XS. In Fig. 6 a breakdown of the lift force during takeoff run for the SS-2 is shown. The estimation was done by using Kuhn's formulas,[2] the coefficient of which was modified by the wind-tunnel data and the flight test results of the UF-XS. The lift by the deflected slip stream is about 80 to 120% of the propeller thrust from V = 0 to 45 knots.

Stability and Control at Low Speeds

The root loci of the stability equation of the UF-XS at C_L = 7.0 are as shown in Fig. 8. The derivatives used are

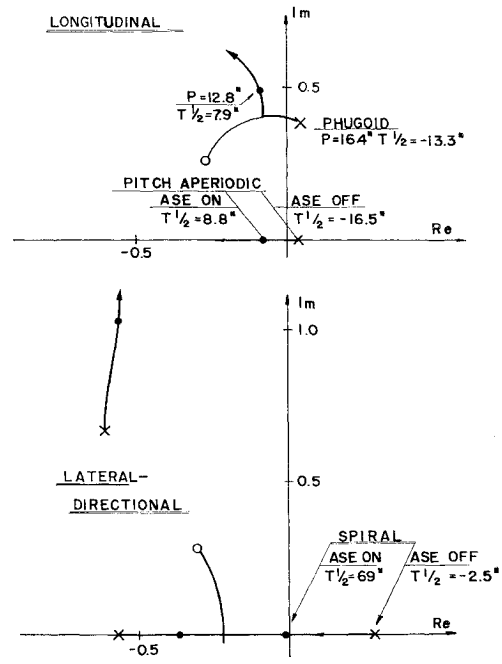

Fig. 8 Stability augmentation.

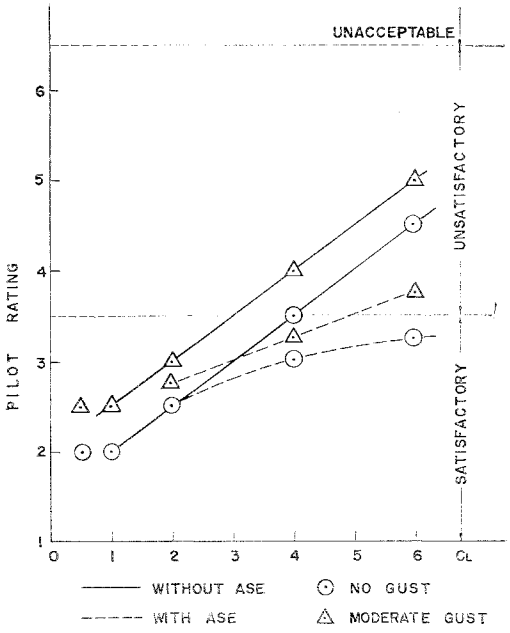

Fig. 9 SS-2 flight simulator pilot rating.

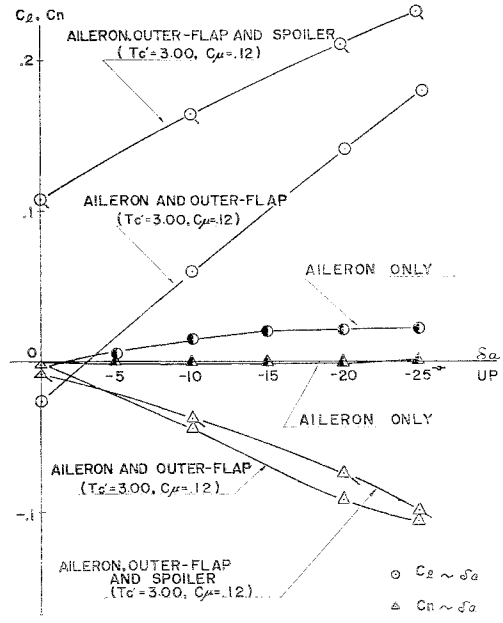

Fig. 10 Aileron effectiveness.

those estimated before the flight test. The inherent stabilities are negative both longitudinally and laterally, as shown by X's in the figures. The period P and the time to half or double amplitude $T^{1/2}$ are added. The very short time to double amplitude (2.5 sec) of the spiral divergence is the main reason for adopting the *ASE*.

The *ASE* moves the three control surfaces as in the following:

$$\delta_{eASE} = K_{oe}(\theta - \theta_0) + K_{1e}\dot{\theta} + K_{sc}\delta_{ep}$$

$$\delta_{aASE} = K_{oa}\phi + K_{1a}\dot{\phi} + K_{sca}\delta_{ap}$$

$$\delta_{rASE} = K_r\delta_{aASE} \qquad K_r \simeq -C_{n\delta a}/C_{n\delta r}$$

The thick lines in Fig. 8 show the stabilization by the *ASE* and the values around the marks shown on the thick lines were tested in the flight tests of the UF-XS, which showed satisfactory flying qualities with *ASE* on except for a side slip excursion at the turn entry.[3]

For the *ASE* of the SS-2, a rudder movement is added to the δ_{rASE} on the advice of Holzhauser (of the NASA Ames Research Center) as a remedy for the side slip excursion,

$$\Delta\delta_{rASE} = -\frac{g}{V_0}\frac{Nr}{N\delta r}\phi + \left(\frac{g}{V_0}\frac{1}{N\delta_r} - \frac{N_p}{N\delta r}\right)p$$

The δ_{rASE} proved effective, as shown in Fig. 9, which represents the pilot rating of the SS-2 by a simulator at the National Aerospace Laboratory, Japan.

Table 2 Control surface deflection

	Deflection in degrees	
Low speed	SS-2	UF-XS
Outboard flaps[a]	up 27, down 18	up 25, down 20
Ailerons	up 27, down 18	up 25, down 20
Spoilers	0–60	0 or 60
Elevators	up 60, down 25	up 45, down 20
Rudder	±45	±45
Cruise		
Outboard flaps	...	...
Ailerons	up 27, down 18	up 25, down 20
Spoilers	...	...
Elevators	up 30, down 12.5	up 22.5, down 10
Rudder	±22.5	±22.5

[a] Engaged with aileron movement.

The maximum deflection of the control surfaces is as shown in Table 2. The lateral control at STOL configuration is the most effective because the outboard flaps and the spoilers are located in the slip stream of the outer engines. The maximum value of the rolling moment coefficient is $C_l = 0.232$, as shown in Fig. 10, which gives an angular acceleration of 0.53 rad/sec^2 at 45 knots. The bank angle at 1 sec after the full control movement is 11.2°, which is less than the 15° recommended by the NASA TN D-331.[4] There are some arguments that the 15° could be somewhat reduced for STOL airplanes. Our experiences with the flight tests of the UF-XS and the simulator test of the SS-2 indicate that 8° to 10° may be acceptable. The rudder is effective, as shown in Fig. 11, for the whole range of deflection (45°, Table 2) at C_μ of 0.03 for the SS-2 (Table 1).

Pitching Moment

Figure 12 shows the pitching-moment coefficient Cm at zero elevator angle vs lift coefficient C_L on the UF-XS. The

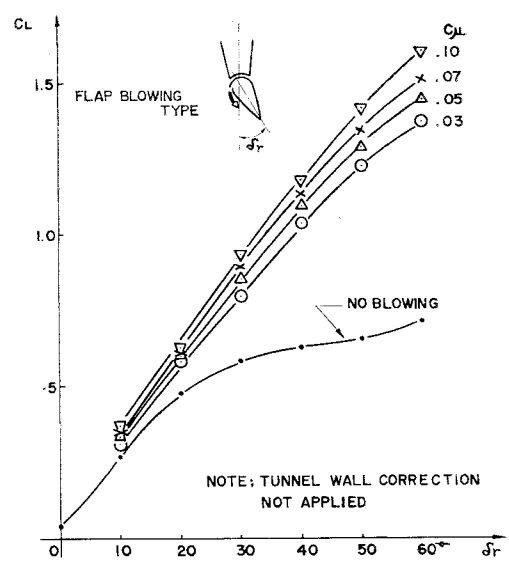

Fig. 11 Lift produced by rudder (wind-tunnel test).

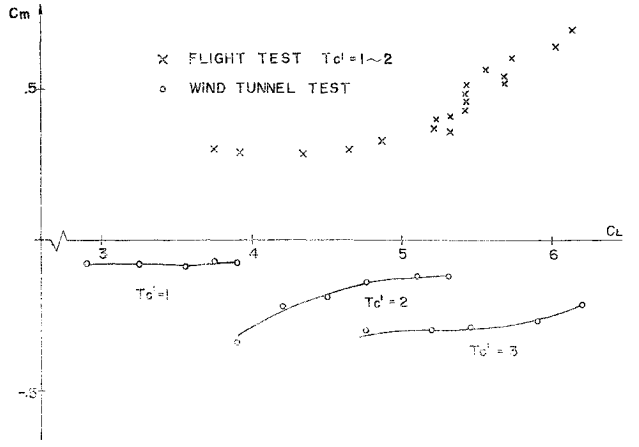

Fig. 12 Pitching-moment discrepancy between flight and wind-tunnel test.

flight tests show nose-up moment equivalent to an elevator deflection of about 13° compared with the wind tunnel results. The wind tunnel used was an 8-ft-diam open section type, and most tests were made at 28 fps wind speed. The model with BLC and running propellers had a span of 80% of the tunnel diameter. No wall correction was applied to the results. The discrepancy is caused mainly by the wall effect.

Asymmetric Characteristics

Figure 13 shows the side-force coefficient $C_Y = Y/qS$ vs lift coefficient $C_L = L/qS$ for the UF-XS. The agreement between wind-tunnel and flight test is good. To investigate the cause of this phenomenon, a pressure distribution survey was made in the wind tunnel, and it was found that the main portion contributing to the side-force is nacelles (Fig. 14). This pressure distribution on the nacelles is understood by the combination of clockwise circulation around the nacelle (viewed from behind) caused by like-rotation propellers with a strong up-wash flow in front of the wing (Fig. 3).

In the SS-2 design nacelles were lowered relative to the wing (Fig. 15) because the nacelle side area above the extension of the wing chord line is mainly generating the side force. The wing was raised relative to the hull to keep the propeller tip clearance above the water. The wind-tunnel tests show that this modification resulted in a remarkable decrease in the side force (Fig. 15) as well as the nose-down pitching moment at takeoff configuration. A nacelle fence,

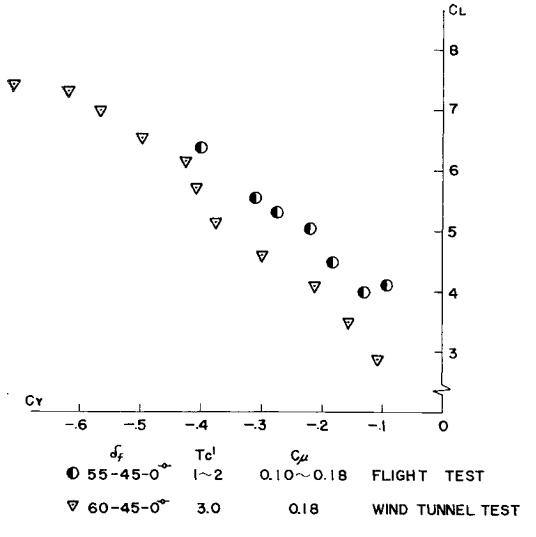

Fig. 13 $C_Y \sim C_L$ UF-XS wind-tunnel test and flight test.

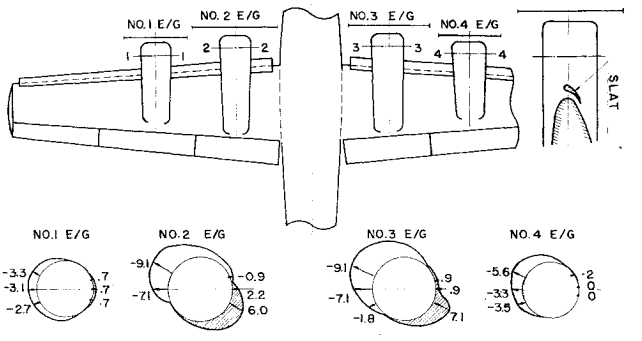

Fig. 14 Pressure distribution ($\Delta p/q_\infty$) on nacelles, $Tc' = 3.0$ (takeoff), UF-XS.

which was set on the nacelle longitudinally at a ten-o'clock position (viewed from behind), was very effective (Fig. 15, nos. 3 and 4) in canceling the sideforce in the wind tunnel, but this is considered unnecessary for the SS-2. Figure 16 shows the improvement in the lateral characteristics; leftward roll and yaw tendency also is improved.

Aileron Droop and Spoilers

The aileron droop originally adopted in the UF-XS was canceled because of the poor effectiveness for the lift augmentation. The spoilers just ahead of ailerons on the UF-XS also showed very little effectiveness, and, for the SS-2 design, they were shifted inward to the position in the outboard propeller slip stream. Wind-tunnel test results (Fig. 10) show a remarkable contribution of the spoilers to the control effectiveness without adverse yaw penalty.

Performance

The takeoff and landing performances are stated in Table 3 together with those of a typical conventional flying boat of similar size. The lift caused by propeller slipstream reaches almost 50% of the total lift of the SS-2 (Fig. 6), and at the same time the induced drag caused by the previously mentioned slip stream lift cancels the total thrust by about one half (Fig. 17). This means that a considerable thrust also is necessary for landing. Figure 18 shows the slow speed performance of the UF-XS predicted by wind-tunnel (no

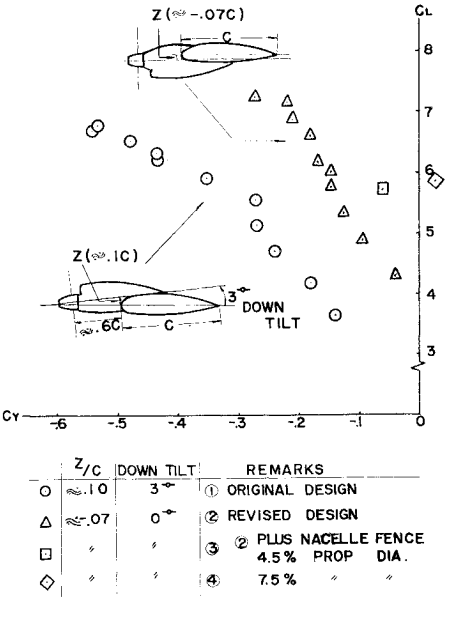

Fig. 15 $C_Y \sim C_L$ SS-2 wind-tunnel test (takeoff configuration).

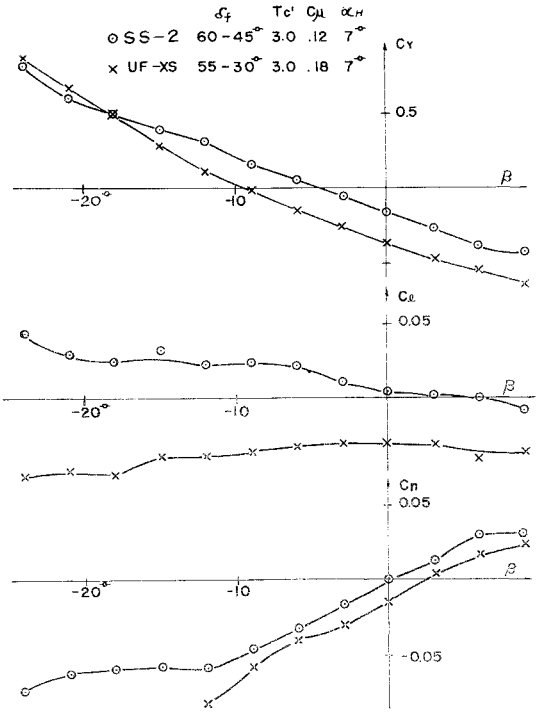

Fig. 16 Lateral characteristics.

wall correction) together with the flight test data (through interpolation and extrapolation). The difference of the angle of attack between the two is from 2° to 4°, which is attributed to the tunnel wall effect.

Figure 19 shows the measured takeoff speed vs applied power of the UF-XS and the predicted value. The flight tests show lower speeds that may be caused by wind-tunnel wall effect, including the ground effect, and the pilot takeoff technique. Figure 20 is the measured takeoff speed and time vs takeoff weight for the UF-XS, together with the calculated values, the formulas of which were modified to take account of the flight test results. The weight corresponding to the SS-2 open ocean gross weight is marked on the figure.

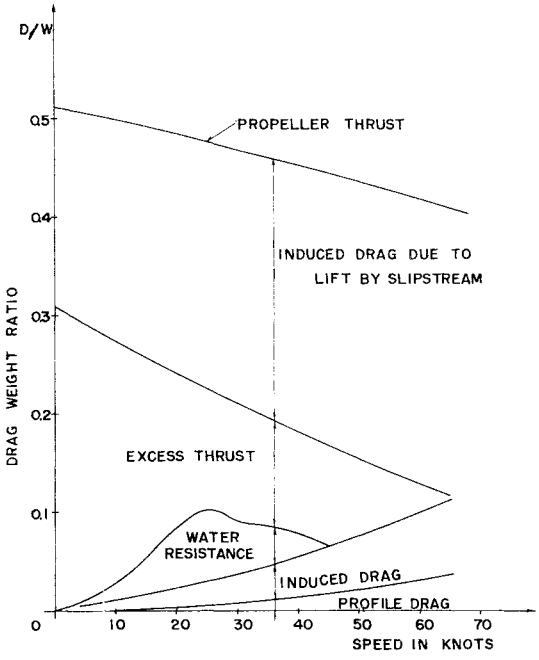

Fig. 17 Drag break down, flap angle = 60-45-0, takeoff speed = 45 knots.

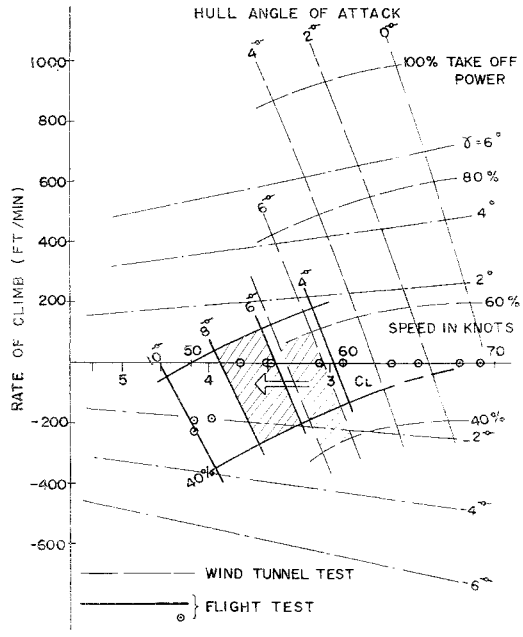

a) δf = 40-30-0, W = 30,000 lb, SL, international standard atmosphere (ISA)

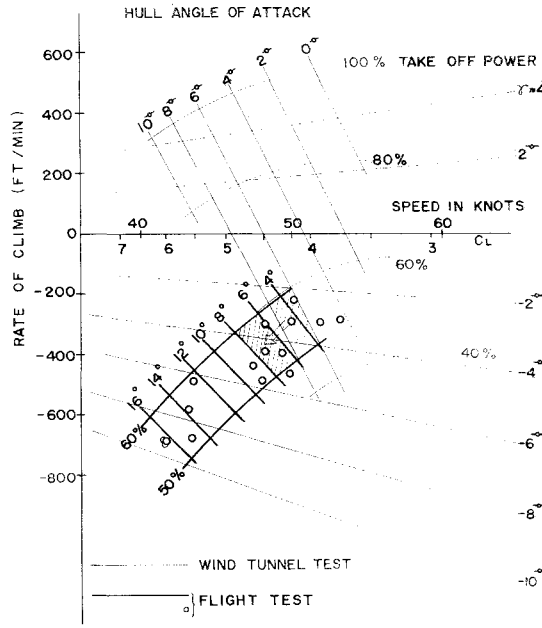

b) δf = 60-45-0, W = 30,000 lb, SL, ISA

Fig. 18 Flight performance of UF-XS.

Table 3 Takeoff and landing performance

	SS-2	Conventional flying boat
Takeoff:		
speed, knots	45	72
L_0/W^a	0.50	0.28
Time, sec	12	35
Run, ft	300	1800
Landing:		
speed, kt	45	85
L_0/W	0.50	0.05
Time, sec	12	...
Run, ft	430	2300
Wing loading, lb/ft²	50	55
Power loading, lb/hp	6.3[b]	12

[a] L_0 = lift caused by propeller slip stream; W = airplane weight.
[b] Corresponding to open ocean G. W.

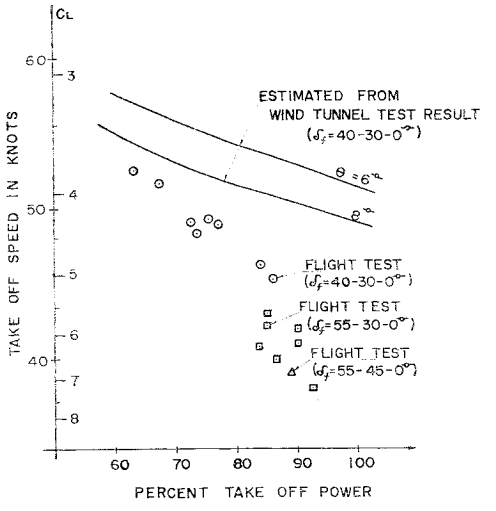

Fig. 19 Takeoff performance of UF-XS reduced to W = 30,000 lb, SL, ISA.

Open Ocean Capability

Among several factors essential for the open ocean capability, slow speed with good flying qualities, impact load, spray, control effectiveness, tip float capacity, longitudinal trim stability, etc., have been proved satisfactory as described in the preceding chapters. With this background the one remaining important factor, the jumping, thrown up by waves, digging into wave crests, or having hard impact, was taken as a criterion for open ocean capability. The towing tank tests in waves show that no jumping is the sufficient condition for takeoff and landing capability, and whether a hull jumps or not under a given sea condition is predicted by a comparatively simple theory.‡

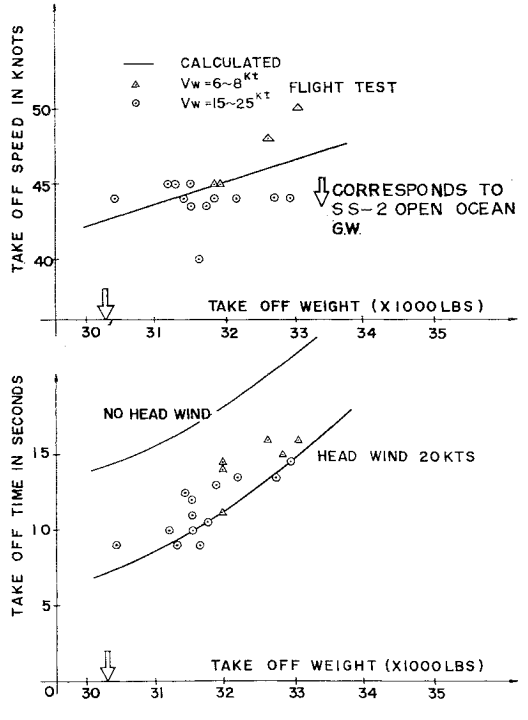

Fig. 20 Takeoff performance of UF-XS, flap angle = 55-30-0.

‡ The theory assumes that a seaplane jumps when the binding force necessary to keep the seaplane mass along the contour of a wave exceeds the load-on-water (weight minus air lift).

Table 4 Calculated utilization

Wind speed knots	Frequency, %	Utilization, %, in each wind speed class: SS-2	Utilization, %, in each wind speed class: Conventional flying boat	Utilization, %, in 1 yr: SS-2	Utilization, %, in 1 yr: Conventional flying boat
Calm	0.83	100.00	100.00	0.83	0.83
0–5	9.97	97.56	89.57	9.72	8.93
5–10	27.34	94.38	71.08	25.83	19.44
10–15	20.85	89.49	46.04	17.67	9.62
15–20	19.94	87.91	25.44	17.54	5.08
20–25	10.30	87.64	17.95	9.03	1.84
25–30	6.66	91.08	0	6.07	0
30–40	3.48	0	0	0	0
40–	0.63	0	0	0	0
Total	100.00	...	...	86.69	45.74

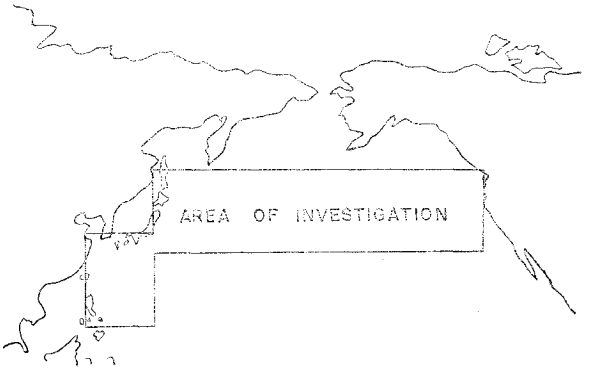

Concerning the structural strength, the water loads were estimated by water tank tests and theoretical calculations, assuming 12-ft waves with length-to-height ratio from 20 to 40 and takeoff and landing speed of 45 knots under wind speeds up to 25 knots. The structural strength thus decided on was checked over the whole sea state range where the operation is capable of being held (according to the jump criterion mentioned previously, i.e., utilizable area in Fig. 5).

Figure 5 is one of the figures prepared from the observed sea state data reported by ships and accumulated for four years in a sea area shown in Table 4. In Fig. 5 the relative occurrence probability is shown, by the shaded area, of a sea state (wave height and wave length or period) under a wind speed of 15–20 knots. The figure shows that a wave

Table 5 Difference of water speed

	SS-2, knots	Conventional flying boat, knots
Head wind	20	20
Takeoff air speed	45	72
Takeoff water speed	25	52
Landing air speed	45	85
Landing water speed	25	65

height between 3 to 7 ft accompanied by a wave length of 100 to 300 ft will most frequently occur at this wind speed range. Also in Fig. 5 utilizable envelopes are drawn which show the limit line of possible jumping for the SS-2 and for a conventional flying boat (Table 3). The utilization is counted on the graph to be 87.9 and 25.4%, respectively, for the specific wind speed range of 15–20 knots. The large difference between the two is because of 1) difference of water speed, Table 5 (also see Table 3); and 2) the difference of lift produced by propeller (L_0 in Table 3) which is to vanish after touch down, as mentioned in "Hydrodynamics."

The utilization limit lines for other wind speeds were obtained by the same procedure. Table 4 shows the total utilization, Fig. 5 being an example for the wind speed class of 15–20 knots of which the frequency is 19.94%. The utilization through the year comes out to be 86.7% for the SS-2 and 45.7% for the conventional flying boat.

References

[1] Kikuhara, S., "A study of spray generated by seaplane hulls," J. Aerospace Sci. **27**, 415–428 (1960).

[2] Kuhn, R. E., "Semi-empirical procedure for estimating lift and drag characteristics of propeller-wing-flap configurations for vertical-and-short-take-off-and landing airplanes," NASA Memo. 1-16-59L (February 1959).

[3] Holzhauser, C. A., Innis, R. C., and Vomaske, R. F., "A flight and simulator study of the handling qualities of a deflected slipstream STOL seaplane having four propellers and boundary layer control," NASA TN D-2964 (June 1965).

[4] Anderson, S. B., "An examination of handling qualities criteria for V/STOL aircraft," NASA TN D-331 (July 1960).

SEPT-OCT. 1966 J. AIRCRAFT VOL. 3, NO. 5

V/STOL Hover Control System Analysis

WILLIAM T. STEILS JR.*
Wright-Patterson Air Force Base, Ohio

The results of a study of the propulsion system/control system interface for several V/STOL hover control concepts in aircraft using the lift plus lift cruise propulsion concept are presented. The control concepts included are proportional reaction controls using lift engine compressor bleed air, engine thrust modulation, and engine thrust vectoring. The effects on control system performance of reaction control thrust augmentation by duct burning are shown. These control concepts are applied to three subsonic V/STOL strike-reconnaissance fighter aircraft of different gross weights, and a comparison of the concepts on the basis of bleed air requirements, thrust-to-weight ratio penalties, and lift engine operating limitations is made. It is shown that the use of duct burning augmentation and engine thrust vectoring control concepts produce significant performance improvements and simplifies lift engine design requirements.

Nomenclature

M = control moment required, lb-ft
I = moment of inertia, slug-ft^2
$\ddot{\theta}$ = required initial angular acceleration, rad/sec^2
ϕ = thrust vector angle for yaw control by engine thrust vectoring, deg
T = total vertical thrust, lb
W = aircraft vertical takeoff gross weight, lb

Introduction

THE majority of the methods currently proposed to provide hover and low-speed control for V/STOL aircraft involve use of the propulsion system either as the primary control thrust producer or as a source of bleed air for separate reaction controls. The use of the propulsion system as part of the control system creates a number of control system/propulsion system interface problems unique to V/STOL aircraft. This paper presents the results of a study of the propulsion system/control system interface for several V/STOL hover control concepts in aircraft using the lift plus lift-cruise propulsion concept. The two primary goals of the study were to determine the effect of control system requirements on lift engine design and to investigate methods of reducing the aircraft design and performance penalties associated with providing hover control.

Presented as Preprint 65-799 at the AIAA/RAes/JSASS Aircraft Design and Technology Meeting, Los Angeles, Calif., November 15–18, 1965; submitted December 16, 1965; revision received March 28, 1966.

* First Lieutenant, Aerospace Engineer, Stability and Control Branch, Systems Engineering Group, Research and Technology Division.

Aircraft

Preliminary designs for three V/STOL strike-reconnaissance fighter aircraft using the lift plus lift-cruise propulsion concept were prepared to provide realistic configuration, weight, and inertia information and to permit evaluation of engine and control system installation factors such as volume limitations and bleed air duct lengths. The three aircraft are shown in Figs. 1–3. The aircraft were designed for three different length missions, so that the resulting differences in their gross weights could be used to evaluate the sensitivity of control system parameters to gross weight and inertia. The aircraft design gross weights were 20,000 lb, 30,000 lb, and 40,000 lb.

Engines

The lift turbojet information used for the study was supplied by Continental Aviation and Engineering Corporation. Three lift engine designs of the same thrust class designed for 0, 6, and 10% of compressor airflow bleed capacity were used for each of the three aircraft, in order to vary the continuous bleed airflow supply for the reaction control system. Each of the three lift engines used the same compressor, and variations in bleed air capacity were obtained by resizing the turbine stage. The effects of altering the design point bleed of the lift engine are indicated in Fig. 4. This figure is intended to show typical characteristics only and does not represent any particular engine used in the study.

As the terms are used in this paper, "continuous" bleed refers to operation at the design point bleed capacity of the engine, and "demand" bleed refers to engine operation at greater than design point bleed or above the turbine inlet temperature limit line. Thus, bleeding any air from the zero